The Canadian Mineralogist
Vol. 54, pp. 461-473 (2016)
DOI: 10.3749/canmin.1500021

MULTI-ANALYTICAL CHARACTERIZATION OF MINERALS OF THE BOWIEITE–KASHINITE SERIES FROM THE SVETLY BOR COMPLEX, URALS, RUSSIA, AND COMPARISON WITH WORLDWIDE OCCURRENCES

Federica ZACCARINI[§]

Department of Applied Geosciences and Geophysics, University of Leoben, Peter Tunner str. 5, A–8700 Leoben, Austria

Luca BINDI

Dipartimento di Scienze della Terra, Università degli Studi di Firenze, via La Pira 4, I–50121 Firenze, Italy

Evgeny PUSHKAREV

Institute of Geology and Geochemistry, Ural Division of Russian Academy of Sciences, Str. Pochtovy per. 7, 620151 Ekaterinburg, Russia

Giorgio GARUTI and Ronald J. BAKKER

Department of Applied Geosciences and Geophysics, University of Leoben, Peter Tunner str. 5, A–8700 Leoben, Austria

Abstract

Grains of the bowieite–kashinite solid-solution series were characterized by electron microprobe analysis, single-crystal X-ray diffraction, and Raman spectroscopy. The grains were recovered from dunitic rocks located in the Svetly Bor Ural-Alaskan type massif, Urals, Russia. Bowieite and kashinite occur as small inclusions (up to 100 μm in size) in isoferroplatinum grains up to 1 mm in diameter. Single-crystal X-ray diffraction data for two selected grains, with compositions $(Rh_{1.16}Ir_{0.82}Cu_{0.02})_{\Sigma 2.00}S_{3.00}$ and $(Ir_{1.06}Rh_{0.87}Cu_{0.04})_{\Sigma 1.97}S_{3.03}$, confirm that the minerals are orthorhombic with similar cell dimensions: *a* 8.46(1), *b* 6.00(1), *c* 6.14(1) Å for bowieite, and *a* 8.46(1), *b* 5.99(1), *c* 6.14(1) Å for kashinite. The Raman spectra of the same two single grains show similar characteristic bands. One grain with composition $(Ir_{0.26}Rh_{0.13}Pt_{0.12}Ni_{0.18}Cu_{0.18}Fe_{0.11})_{\Sigma 0.98}S$ was found associated with the kashinite. It shows a distinctive Raman spectrum and may represent a new platinum-group mineral, although the small size (less than 20 μm) prevented us from obtaining X-ray diffraction data. Our data for the bowieite–kashinite series are compared with selected worldwide occurrences.

Keywords: bowieite–kashinite series, X-ray diffraction, Raman spectroscopy, electron microprobe, Svetly Bor, Urals, Russia.

Introduction

The presence of a possible solid-solution series between bowieite (ideally Rh_2S_3) and kashinite (ideally Ir_2S_3), two rare platinum-group minerals (PGM), was postulated by Hansen & Anderko (1958) about 60 years ago on the basis of synthetic counterparts and later by Parthé *et al*. (1967). In spite of the significant number of reports of natural occurrences of minerals of the bowieite–kashinite solid-solution series, few data are available about their chemical compositions. So far, only the grains from the type localities and one grain from China have been studied by X-ray diffraction (Chen *et al*. 1981, Desborough & Criddle 1984, Begizov *et al*. 1985). Furthermore, members of the bowieite–kashinite series

[§] *Corresponding author e-mail address*: Federica.Zaccarini@unileoben.ac.at

have never been investigated by Raman spectroscopy. Here we present, for the first time, single-crystal X-ray diffraction, Raman spectra, and results of electron-microprobe analyses of selected grains, including an intermediate composition in the bowieite–kashinite series from a dunite of the Svetly Bor massif, central Urals, Russia. The obtained compositions are compared with chemical data from other occurrences worldwide.

Previously Described Occurrences

Begizov *et al*. (1975) were the first to describe a natural occurrence of $(Rh,Ir)_2S_3$ from ultramafic rocks associated with the Gusevogorskiy Complex in the Urals. Cabri *et al*. (1981) reported on the presence of unnamed Rh_2S_3 as a small inclusion in a Pt–Fe alloy nugget from Ethiopia. However, in both these occurrences, the grains were found to be too small to allow X-ray characterization. Subsequently, Chen *et al*. (1981) attempted the X-ray study of a Rh_2S_3 phase from the concentrically zoned mafic-ultramafic Gaosital Complex in China. This Rh_2S_3 phase, however, was officially accepted as a new mineral with the name bowieite only four years later (Desborough & Criddle 1984). The type locality of bowieite is Goodnews Bay in Alaska, where the new mineral was found included in Pt–Fe nuggets. Since its official discovery, more than 20 occurrences of bowieite have been documented and in most of them bowieite occurs as inclusions in Pt–Fe nuggets associated with placer deposits (Atanasov 1990, Hagen *et al*. 1990, Johan *et al*. 1991, Slansky *et al*. 1991, Augé & Legendre 1992, Legendre & Augé 1992, Weiser & Schmidt-Thomé 1993, Gornostayev *et al*. 1999, Podlipskii *et al*. 1999, Britvin *et al*. 2001, Sidorov *et al*. 2004, Barkov *et al*. 2005, Melcher *et al*. 2005, Stanley *et al*. 2005, Oyunchimeg *et al*. 2009, Fedortchouk *et al*. 2010, Zaccarini *et al*. 2013, Airiyants *et al*. 2014). Bowieite has also been reported to occur in banded chromitite associated with ophiolites from Canada and Austria (Corrivaux & Laflamme 1990, Malitch *et al*. 2001, 2003). It has also been encountered in a Ni-rich laterite in the Dominican Republic, as an inclusion in a disseminated chromite grain (Aiglsperger *et al*. 2015), in an ultramafic lens in a granite gneiss in India (Devaraju *et al*. 2004), and in magnetite-bearing gabbros from the Freetown Layered Complex of Sierra Leone (Bowles *et al*. 2013).

Kashinite was first described by Begizov *et al*. (1985) from the Niznhy Tagil Ural-Alaskan type Complex, located in the central Urals of Russia. It was then reported as inclusions in chromite crystals from several chromitites associated with ophiolites or lherzolite complexes (Legendre & Augé 1986, Garuti *et al*. 1999, Malitch *et al*. 2001, 2003, Power & Pirrie 2004, Zaccarini *et al*. 2004, Uysal *et al*. 2009, González-Jiménez *et al*. 2011, Pašava *et al*. 2011). More rarely, kashinite has been found included in chromite grains of Ural-Alaskan type chromitite (Garuti *et al*. 2002, 2003, Zaccarini *et al*. 2013), from placer deposits (Hagen *et al*. 1990, Johan *et al*. 1991, Slansky *et al*. 1991, Podlipskii *et al*. 1999, Weiser & Bachmann 1999, Britvin *et al*. 2001, Zaccarini *et al*. 2013), and from sulfide-poor ore (Gabov 2010).

Fig. 1. View of the trench in the Svetly Bor massif from which the analyzed dunite was collected.

Sample Provenance and Methodology

Our samples were collected from an exploration trench in the Svetly Bor massif (Fig. 1), which is located in the Urals, about 250 km NW of Ekaterinburg (Figs. 2A, B). The Svetly Bor massif is one of the concentrically zoned Ural-Alaskan type complexes that occur in the platinum-bearing belt exposed in the central-northern part of the Ural orogen, east of the main Uralian Fault (Figs. 2A, B). The platinum-bearing belt extends for more than 1000 km in the central and northern Urals (lat. 58° to 68°N). The Svetly Bor massif occurs west of the Kachkanar Complex, which is composed of wehrlite, clinopyroxenite, different gabbros, and norite (Fig. 2C). Svetly Bor consists of a dunite core enveloped by a narrow rim composed of wehrlite and clinopyroxenite (Fig. 2C). Several hornblendite dikes cut across the dunite, which commonly contains schlieren and veins of chromitite. The investigated samples were collected from a dunite in the southwestern portion of the massif (Fig. 2C) that contains only disseminated grains of Cr-rich spinel and no segregation of chromitite. The dunite sample was crushed and washed on a concentration table. As it may contain coarse grains of PGM (Zaccarini *et al*. 2013), the PGM were hand-picked under a binocular microscope. Sixteen PGM

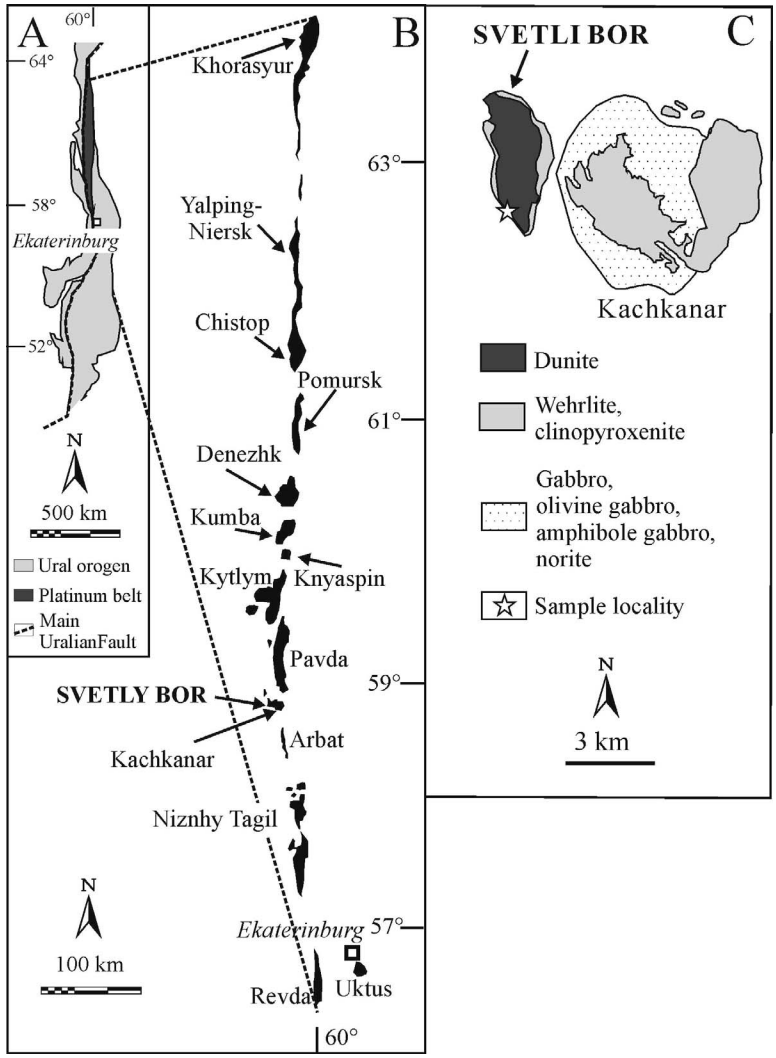

FIG. 2. Simplified geological setting of the platinum-bearing Belt within the Ural orogen (A), showing the location of the major Ural-Alaskan-type complexes (B) (simplified after Yefimov *et al.* 1993). (C) Geological map of the Svetly Bor and Kachkanar massifs, showing the sample location.

grains were selected, studied by reflected-light microscopy, and then mounted in epoxy blocks and polished.

The grains were analyzed with a JEOL JXA 8200 electron microprobe in the Eugen Stumpfl laboratory at the University of Leoben, Austria. The instrument operated in the both EDS and WDS modes, with an accelerating voltage of 20 kV and a beam current of 10 nA, and a beam diameter of about 1 μm. The counting times on peak and backgrounds were 20 and 10 seconds, respectively. The X-ray lines used were: $K\alpha$ for S, Fe, Cu, and Ni; $L\alpha$ for Ir, Ru, Rh, Pd, and As; and $M\alpha$ for Os. The following diffracting crystals were selected: PETH for S, Ru, Os, Rh, and Pd; LIFH for Fe, Ni, and Ir; and TAP for As. For standard materials, we used pure metals for the platinum-group elements (PGE, *i.e.*, Os, Ir, Ru, Rh, Pt, and Pd), and nickeline, pyrite, and chalcopyrite for Fe, Cu, Ni, S, and As. Selected compositions of PGM are listed in Tables 1, 2, and 3.

The Raman spectra were collected using a LABRAM (ISA Jobin Yvon) instrument at the University of Leoben. A frequency-doubled 100 mW Nd-YAG laser with an excitation wavelength of $\lambda =$

TABLE 1. SELECTED ANALYSES OF ISOFERROPLATINUM FROM THE SVETLY BOR DUNITE

wt.%	Os	Ir	Ru	Rh	Pt	Pd	Fe	Ni	Cu	S	As	Total
PtFeB-1	0.00	2.88	0.00	0.63	87.98	0.58	8.13	0.00	0.65	0.08	0.00	100.91
PtFeB-2	0.00	3.28	0.04	0.48	86.98	0.47	7.93	0.04	0.58	0.07	0.02	99.88
PtFeB-3	0.00	3.71	0.00	0.55	86.56	0.50	7.80	0.00	0.54	0.07	0.00	99.73
PtFeB-4	0.00	1.68	0.00	0.47	89.13	0.68	8.16	0.03	0.60	0.06	0.00	100.81
PtFeB-5	0.00	2.69	0.00	0.53	88.15	0.76	8.05	0.00	0.63	0.08	0.02	100.91
PE1395G1-4	0.00	2.39	0.00	0.57	89.34	0.08	7.68	0.03	1.06	0.05	0.00	101.21
PE1395G2-2	0.00	1.90	0.07	0.63	89.51	0.23	7.73	0.00	1.05	0.00	0.00	101.12
PE1395G3-1	0.00	1.99	0.00	0.84	88.37	0.45	7.46	0.01	1.01	0.07	0.00	100.20
PE1395G3-6	0.00	1.92	0.03	0.82	89.15	0.41	7.66	0.03	1.05	0.09	0.01	101.18
PE1395G4-1	0.00	2.04	0.05	0.66	88.93	0.52	7.81	0.00	1.02	0.08	0.00	101.10
PE1395G4-3	0.00	1.84	0.04	0.82	89.29	0.49	7.70	0.03	1.09	0.03	0.00	101.33
PE1395G4-4	0.00	2.19	0.00	0.67	89.13	0.56	7.64	0.00	1.03	0.06	0.01	101.28
PE1395G4-5	0.59	2.69	0.11	0.94	87.22	0.46	7.46	0.03	0.94	0.04	0.01	100.48
PE1395G5-1	0.06	2.18	0.10	0.68	89.04	0.56	7.85	0.02	0.97	0.07	0.00	101.52
PE1395G5-3	0.00	2.08	0.03	0.75	89.07	0.46	7.94	0.01	0.99	0.09	0.00	101.40
PE1395G6-1	0.28	2.38	0.11	0.75	88.39	0.51	7.65	0.01	1.06	0.07	0.00	101.21
PE1395G6-3	0.18	1.82	0.02	0.65	88.97	0.54	7.85	0.00	0.94	0.05	0.00	101.02
PE1395G6-4	0.00	2.05	0.07	0.73	89.11	0.58	7.75	0.00	0.97	0.06	0.00	101.31
PE1395G6-5	0.00	2.01	0.00	0.73	89.27	0.55	7.69	0.03	0.99	0.08	0.00	101.35
PE1395G7-3	0.00	2.12	0.03	0.75	89.31	0.37	7.52	0.00	0.97	0.07	0.00	101.15
PE1395G7-4	0.00	1.99	0.01	0.64	89.39	0.36	7.69	0.04	0.95	0.05	0.00	101.12
PE1395G7-5	0.37	2.09	0.10	0.78	88.62	0.63	7.83	0.01	0.97	0.07	0.00	101.47
PE1395G8-1	0.09	2.27	0.05	0.63	88.98	0.32	7.82	0.07	0.94	0.06	0.00	101.23
PE1395G8-2	0.25	2.45	0.01	0.72	88.46	0.47	7.62	0.00	0.96	0.07	0.00	101.02
PE1395G8-3	0.00	2.25	0.01	0.74	89.07	0.50	7.74	0.03	0.93	0.10	0.01	101.38
PE1395G8-4	0.00	2.16	0.00	0.75	89.22	0.44	7.68	0.00	0.91	0.09	0.00	101.25
PE1395G8-5	0.00	2.02	0.00	0.65	88.75	0.47	7.69	0.04	0.93	0.07	0.00	100.62
PE1395G9-1	0.00	2.39	0.00	0.96	88.75	0.57	7.58	0.02	0.99	0.02	0.00	101.27
PE1395G9-3	0.00	2.43	0.00	0.87	88.43	0.30	7.66	0.04	0.98	0.05	0.04	100.78
PE1395G9-4	0.00	2.39	0.00	0.95	88.79	0.60	7.68	0.00	0.98	0.05	0.02	101.46
PE1395G9-5	0.00	1.91	0.00	0.88	89.43	0.31	7.94	0.01	0.89	0.08	0.00	101.46
PE1395G10-2	0.00	2.07	0.00	0.87	88.29	0.53	7.81	0.00	0.90	0.04	0.03	100.53
PE1395G10-3	0.00	2.30	0.00	0.96	88.53	0.50	7.80	0.01	0.95	0.09	0.00	101.13
PE1395G10-4	0.00	2.39	0.00	0.93	88.67	0.58	7.66	0.00	1.03	0.02	0.00	101.28
PE1395G10-5	0.00	2.41	0.05	1.02	88.49	0.49	7.82	0.00	0.91	0.04	0.00	101.23
PE1395G11-1	0.00	1.31	0.01	0.55	89.94	0.33	7.82	0.00	0.87	0.04	0.00	100.87
PE1395G11-2	0.30	2.00	0.02	0.39	89.34	0.24	7.84	0.00	0.86	0.12	0.00	101.11
PE1395G11-3	0.00	1.64	0.04	0.47	90.24	0.37	7.75	0.00	0.86	0.09	0.00	101.46
PE1395G11-4	0.00	1.47	0.04	0.50	90.01	0.26	7.75	0.00	0.83	0.04	0.00	100.90

532.068 nm was used. The laser power at the sample surface was about 1 to 2 mW. Both notch-filter (532 nm, blocking relative wavenumbers below 170 cm^{-1}) and edge-filter (532 nm, blocking relative wavenumbers below 80 cm^{-1}) were used to suppress Rayleigh scattering and anti-Stokes scattering. Measurements were carried out with an LMPlanFI 100×/0.8 (Olympus) objective lens. The instrument has a spectral resolution of 1.62 cm^{-1} at low Δv (about 0 cm^{-1}) and of 1.1 cm^{-1} at high Δv (about 3000 cm^{-1}). Additional neutral filters with variable optical densities were used to decrease the laser power to prevent damage or transformation of the samples. We simultaneously measured the emission lines of neon for calibration.

The same crystals used for the Raman investigation were then preliminarily examined with a Bruker-Enraf MACH3 single-crystal diffractometer using graphite-monochromatized Mo$K\alpha$ radiation. A more precise analysis was then carried out by means of a CCD-equipped Xcalibur PX Ultra diffractometer using Cu$K\alpha$ radiation. The data were processed using the *CrysAlis* software package version 1.171.31.2 (Oxford Diffraction 2006) running on the Xcalibur PX control PC.

TABLE 2. SELECTED ANALYSES OF THE UNNAMED PGM FROM THE SVETLY BOR DUNITE

	Ir	Rh	Pt	Fe	Ni	Cu	S	Total
wt.%								
PtFeBrim1	31.69	8.82	17.03	4.06	7.12	7.68	21.10	97.50
PtFeBrim2	34.71	8.72	15.56	4.33	6.82	7.22	21.18	98.55
PtFeBrim3	33.29	8.99	16.54	4.17	6.98	7.53	21.18	98.66
PtFeBrim4	33.71	8.62	16.12	4.29	7.14	7.36	21.08	98.31
PtFeBrim5	33.67	8.84	16.09	4.29	7.19	7.32	21.89	99.28
at.%								
PtFeBrim1	12.58	6.54	6.66	5.54	9.25	9.22	50.20	
PtFeBrim2	13.75	6.45	6.08	5.90	8.85	8.66	50.31	
PtFeBrim3	13.14	6.63	6.43	5.66	9.02	8.99	50.12	
PtFeBrim4	13.35	6.38	6.29	5.85	9.26	8.81	50.05	
PtFeBrim5	13.07	6.41	6.15	5.72	9.14	8.59	50.93	
apfu								
PtFeBrim1	0.50	0.26	0.27	0.22	0.37	0.37	2.01	
PtFeBrim2	0.55	0.26	0.24	0.24	0.35	0.35	2.01	
PtFeBrim3	0.53	0.27	0.26	0.23	0.36	0.36	2.00	
PtFeBrim4	0.53	0.26	0.25	0.23	0.37	0.35	2.00	
PtFeBrim5	0.52	0.26	0.25	0.23	0.37	0.34	2.04	
apfu								
PtFeBrim1	0.25	0.13	0.13	0.11	0.19	0.18	1.00	
PtFeBrim2	0.28	0.13	0.12	0.12	0.18	0.17	1.01	
PtFeBrim3	0.26	0.13	0.13	0.11	0.18	0.18	1.00	
PtFeBrim4	0.27	0.13	0.13	0.12	0.19	0.18	1.00	
PtFeBrim5	0.26	0.13	0.12	0.11	0.18	0.17	1.02	

Results

Mineral description and composition

The members of the bowieite–kashinite series found in the Svetly Bor dunite invariably occur associated with crystals of Pt–Fe that vary in size from 200 μm up to 1 mm (Fig. 3). The host Pt–Fe alloy is chemically homogeneous with an isoferroplatinum-type composition (Fig. 4). The isoferroplatinum contains low concentrations (usually less than 1 wt.%) of Os, Ru, Rh, Pd, Ni, Cu, S, and As, and appreciable amounts of Ir (up to 3.7 wt.%) (Table 1).

The bowieite–kashinite grains vary in size from 10 to 100 μm (Fig. 3). Under reflected light, bowieite and kashinite are pinkish-grey in color and show a weak anisotropy. One grain of bowieite was found associated with laurite (Figs. 3A, B). According to the backscattered electron image (Fig. 3B) and EDS analyses, the bowieite grain is slightly enriched in Ir at the contact with isoferroplatinum. One grain of kashinite is rimmed by an unnamed PGM (Figs. 3C, D) that, according to the microprobe results, may correspond to $(Ir_{0.26}Rh_{0.13}Pt_{0.12}Ni_{0.18}Cu_{0.18}Fe_{0.11})_{\Sigma 0.98}S$ (Table 2). This unnamed PGM is grey in color and darker compared to the associated kashinite, and it is slightly anisotropic. The EDS analyses show that besides the major components Ir, Rh, and S, the grains of bowieite–kashinite from the Svetly Bor dunite contain only small amounts of Cu. Therefore only these elements were quantitatively determined (Table 3). The data obtained were plotted, as at.%, in the triangular diagram presented in Figure 5A. The diagram shows that the analyzed grains contain dominantly Ir and Rh. We note that the two endmembers were not found in the samples studied. Furthermore, the analyzed kashinite displays a limited compositional range, whereas bowieite shows a larger compositional variation (Fig. 5A).

X-ray diffraction data

Two fragments of bowieite and kashinite, each about 100 μm in size, and corresponding to the chemical compositions $(Rh_{1.16}Ir_{0.82}Cu_{0.02})_{\Sigma 2.00}S_{3.00}$ and $(Ir_{1.06}Rh_{0.87}Cu_{0.04})_{\Sigma 1.97}S_{3.03}$, respectively, were extracted from the polished section. The single-crystal X-ray diffraction data confirm that the two selected minerals are orthorhombic. According to the obtained values, *a* 8.46(1), *b* 6.00(1), *c* 6.14(1) Å for bowieite and *a* 8.46(1), *b* 5.99(1), *c* 6.14(1) Å for kashinite, the two phases are not distinguishable. The unit-cell values of the grains we studied from the Svetly Bor

TABLE 3. SELECTED COMPOSITIONS OF KASHINITE–BOWIEITE SERIES FROM SVETLY BOR DUNITE

	Ir	Rh	Cu	S	Total
wt.%					
Kashinite					
PtFeB-1	51.28	22.24	0.59	25.12	99.23
PtFeB-2	51.01	22.50	0.62	24.96	99.09
PtFeB-3	51.01	22.72	0.64	25.04	99.42
PtFeB-4	51.69	22.94	0.65	24.83	100.11
PtFeB-5	51.14	23.08	0.70	24.85	99.77
PtFeB-6	52.38	22.07	0.66	24.91	100.02
PtFeB-7	52.81	21.74	0.69	24.66	99.91
PtFeB-8	53.17	21.96	0.67	24.56	100.36
PtFeB-9	52.27	22.69	0.64	24.75	100.36
PtFeB-10	52.17	23.07	0.63	24.74	100.61
po1395G1-11	54.48	20.88	0.61	24.16	100.13
po1395G1-12	51.45	24.12	0.54	24.07	100.18
po1395G1-18	49.33	25.76	0.56	24.51	100.17
po1395G1-22	49.54	25.98	0.57	24.49	100.59
po1395G1-23	50.08	25.32	0.54	24.73	100.68
Bowieite					
po1395G1-1	39.71	34.29	0.50	26.05	100.54
po1395G1-2	41.60	32.67	0.46	25.26	99.99
po1395G1-3	42.36	31.80	0.45	25.62	100.22
po1395G1-4	43.28	30.66	0.48	24.98	99.41
po1395G1-5	43.49	31.28	0.47	25.13	100.37
po1395G1-7	41.78	32.20	0.47	25.15	99.60
po1395G1-8	41.33	32.74	0.47	25.48	100.02
po1395G1-9	40.27	33.70	0.43	25.66	100.06
po1395G1-10	41.31	32.77	0.41	25.45	99.94
po1395G1-13	47.02	27.08	0.52	24.84	99.47
po1395G1-14	48.76	26.26	0.51	24.54	100.08
po1395G1-15	47.78	26.87	0.55	24.82	100.01
po1395G1-17	47.54	27.33	0.49	24.41	99.77
po1395G1-19	45.43	28.94	0.51	25.11	99.99
po1395G1-20	47.17	27.57	0.56	24.90	100.20
po1395G1-21	48.27	26.34	0.54	24.82	99.97

dunite are listed in Table 4, together with the few data available in the literature. The fact that we observed very close cell parameters for the two studied crystals is not surprising, given the close similarity also observed for the two synthetic endmembers.

Raman spectra

The same grains of bowieite and kashinite used for the diffraction study and the unnamed PGM sulfide mineral were also analyzed by Raman spectroscopy. All these PGM display very well-defined and characteristic spectra in the range of 250 to 400 cm^{-1} (Fig. 6). Interestingly, the bowieite and kashinite spectra are very similar, showing two narrow bands at about 287–308 cm^{-1} and 308–311 cm^{-1} (Figs. 6A, B) and another relatively wider band at about 374 cm^{-1} and 387 cm^{-1}, respectively. They differ from those of the unnamed PGM sulfide mineral (Fig. 6C), which displays only two well-defined bands at about 298 cm^{-1} and 368 cm^{-1}. Several grains of the isoferroplatinum host were also checked by Raman spectroscopy; none of them showed discernible scattering bands, proving that they are Raman-inactive.

Comparison with Bowieite–Kashnite Occurrences Worldwide

An overview of worldwide occurrences of the bowieite–kashinite solid-solution series is given in Table 5. Furthermore, the compositions of bowieite–kashinite from Svetly Bor analyzed in the present work are plotted in terms of Rh-Ir-(Ru+Pt+Pd) (Fig. 5) and compared with compositions taken from the occurrenc-

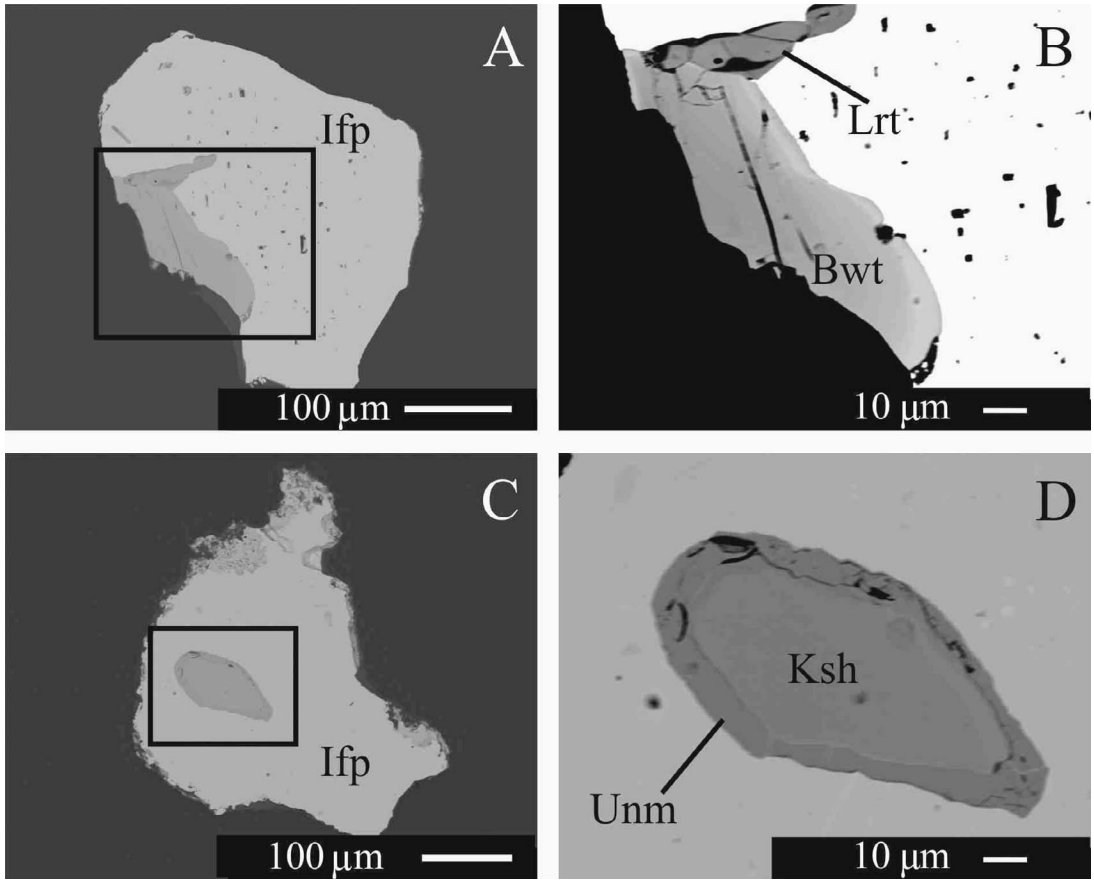

FIG. 3. Backscattered electron (BSE) images showing morphology and mineral assemblages of the PGM included in isoferroplatinum of the Svetly Bor dunite. (A) Grain of bowieite in contact with laurite. (B) Enlargement of A. (C) Grain of kashinite rimmed by an unnamed PGM. (D) Enlargement of C. Abbreviations: Ifp = isoferroplatinum, Lrt = laurite, Bwt = bowieite, Ksh = kashinite, Unm = unnamed $(Ir_{0.26}Rh_{0.13}Pt_{0.12}Ni_{0.18}Cu_{0.18}Fe_{0.11})_{\Sigma 0.98}S$.

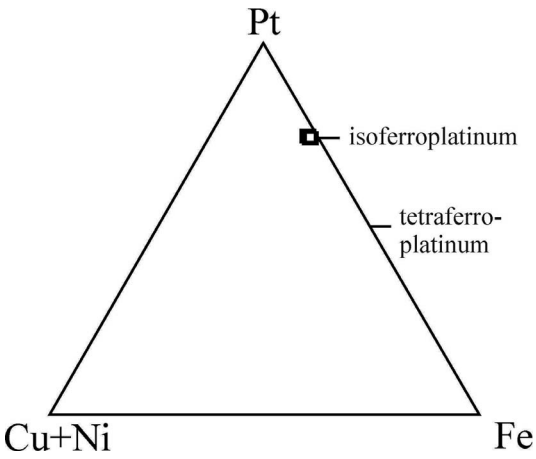

FIG. 4. Plots (at.%) of compositions of the Pt alloys from the Svetly Bor dunite in the triangular diagram Pt–Fe–Cu+Ni.

es listed in Table 5, for which electron-microprobe data are available. The triangular diagram shows that both the bowieite and kashinite analyzed in this contribution (Fig. 5A) differ from the compositions reported from the type localities (Fig. 5B). In particular, bowieite from Goodnews Bay (Desborough & Criddle 1984) is enriched in Pt, and kashinite from Niznhy Tagil analyzed by Begizov *et al*. (1985) is characterized by a much greater range in Ir content (Figs. 5A, B). The bowieite from the Svetly Bor dunite has a composition comparable with those reported from placer deposits in the Yukon Territory, Canada (Fedortchouk *et al*. 2010); eastern Madagascar (Augé & Legendre 1992, Legendre & Augé 1992); Kamchatka (Podlipskii *et al*. 1999, Sidorov *et al*. 2004); and far East Russian (Gornostayev *et al*. 1999), as well as with those described from the Austrian chromitite of Kraubath (Malitch *et al*. 2001,

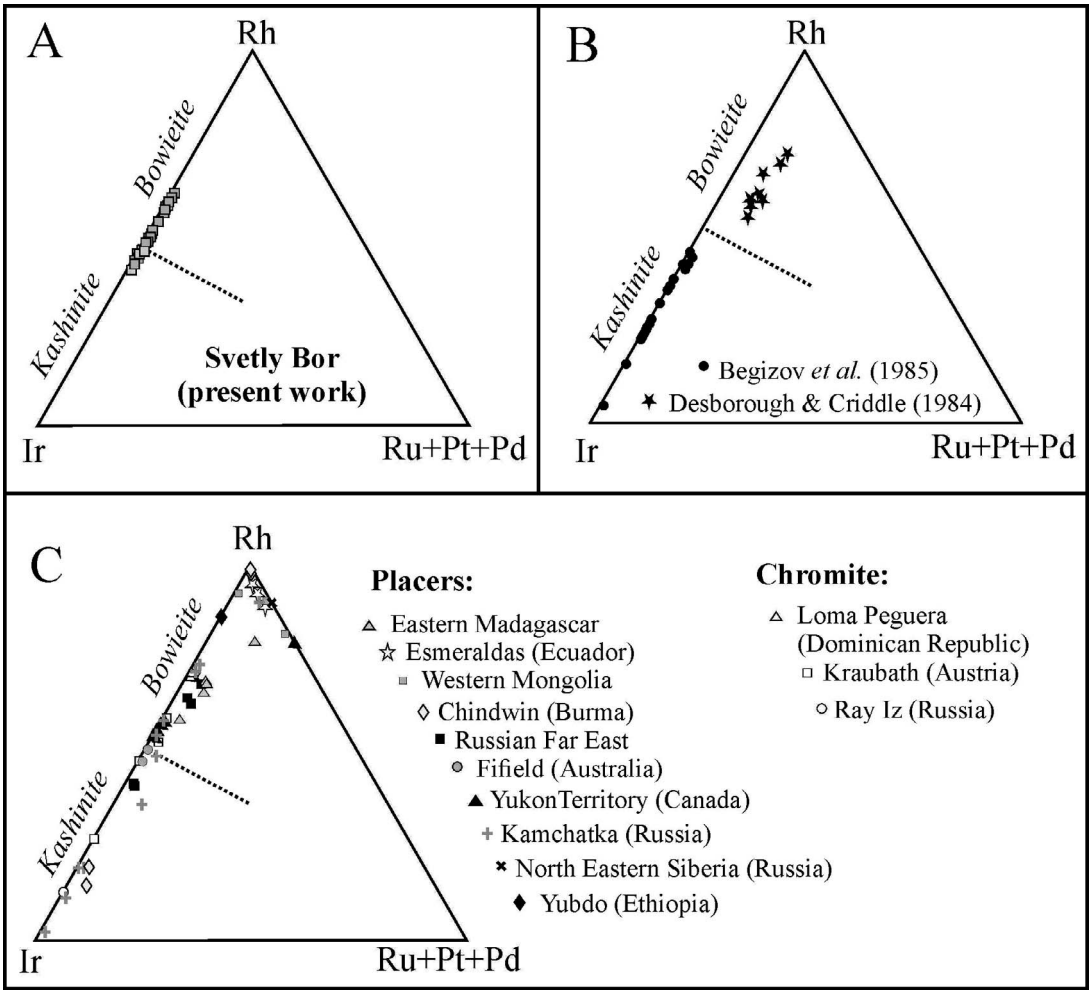

FIG. 5. Plots (at.%) of compositions of the bowieite–kashinite series in the triangular diagram Rh–Ir–Ru+Pt+Pd. (A) Compositions from the Svetly Bor dunite (present work). (B) Compositions from the type localities of bowieite and kashinite. (C) Selected compositional data from the literature.

2003) (Figs. 5A, C). The composition of kashinite from the Svetly Bor dunite resembles those analyzed from nuggets found in Kamchatka (Podlipskii *et al*. 1999, Sidorov *et al*. 2004), in Australia (Johan *et al*. 1991, Slansky *et al*. 1991), and from Kraubath chromitite (Malitch *et al*. 2001, 2003) (Figs. 5A, C). The triangular diagrams presented in Figure 5 show that endmember bowieite and kashinite have been only reported from placer deposits in Burma (Hagen *et al*. 1990) and Kamchatka (Sidorov *et al*. 2004) (Fig. 5C). The same diagrams also confirm the existence of an almost complete solid-solution series between the two end-members. Although the main substitution in the bowieite–kashinite solid-solution series involves the isovalent exchange of Rh and Ir, as is shown by the grains analyzed in this contribution (Fig. 5A), several compositions that plot in the field of bowieite are characterized by concentrations of Ru, Pt, and Pd higher than those of Ir (Fig. 5C). In particular, bowieite analyzed in the nuggets from Ecuador contains up to 2.32 at.% Pt and 0.92 at.% Ru (Weiser & Schmidt-Thomé 1993) and one analysis of a sample from north-eastern Siberia (Airiyants *et al*. 2014) shows 2.66 at.% Ru and 0.6 at.% Pt. Bowieite from the alluvial deposits of Madagascar (Augé & Legendre 1992) contains up to 4.05 at.% Pd. High amounts of Pt (up to 7.28 at.%) and Pd (up to 1.32 at.%) have been reported in bowieite from placers in the Yukon Territory, Canada

TABLE 4. CELL PARAMETERS FOR BOWIEITE–KASHNITE

Provenance	A	B	C	Ref.
bowieite				
Svetly Bor	8.46(1)	6.00(1)	6.14(1)	p.w.
Synthetic	8.462(3)	5.985(2)	6.138(2)	1
Type locality	8.454(7)	6.002(7)	6.121(8)	2
	8.454(4)	6.002(5)	6.122(9)	2
China	8.493	5.987	6.167	2
kashinite				
Svetly Bor	8.46(1)	5.99(1)	6.14(1)	p.w.
Synthetic	8.465(2)	6.011(2)	6.149(2)	1
Type locality	8.464	6.001	6.146	3

p.w. = present work, Ref.: 1 = Parthé *et al.* 1967, 2 = Desborough & Criddle 1984, 3 = Begizov *et al.* 1985.

(Fedortchouk *et al*. 2010). Bowieite from the placer deposits of Kamchatka (Sidorov *et al*. 2004) and Western Mongolia (Oyunchimeg *et al*. 2009) is slightly enriched in Pt, up to 2.77 at.% and 2.89 to 4.49 at.%, respectively.

Concluding Remarks

On the basis of a multi-analytical characterization of minerals belonging to the bowieite–kashinite solid-solution series from the Svetly Bor dunite and comparison with worldwide occurrences, the following conclusions can be drawn:

Bowieite and kashinite cannot be distinguished on the basis of X-ray diffraction owing to the similarity of the cell parameters (Table 4).

Bowieite, kashinite, and the unnamed $(Ir_{0.26}Rh_{0.13}Pt_{0.12}Ni_{0.18}Cu_{0.18}Fe_{0.11})_{\Sigma 0.98}S$ phase show characteristic Raman bands (Fig. 6). Their spectra are different from those previously reported for other PGM sulfides, such as laurite, erlichmanite, and an unnamed Ir-Rh-Ni-Fe-Cu sulfide mineral from a chromitite in Costa Rica (Zaccarini *et al*. 2010). Therefore, the PGM investigated in this work can be distinguished using Raman spectroscopy. However, the spectra of bowieite and kashinite are quite similar, probably due to the fact that the analyzed grains have a limited Rh:Ir ratio. The Raman spectra are sensitive to the presence of covalent bonding (Turrel 1996), producing a very well-defined and visible spectrum in the material in which this type of bond is present (Zaccarini *et al*. 2010, Vymazalová *et al*. 2012, 2014). Therefore, we contend that the investigated PGM sulfides of Svetly Bor are characterized by the presence of covalent bonding. Isoferroplatinum, however, displays a flat Raman spectrum, thus suggesting that the possible bonds present in this PGM are metallic or ionic, as previously reported for

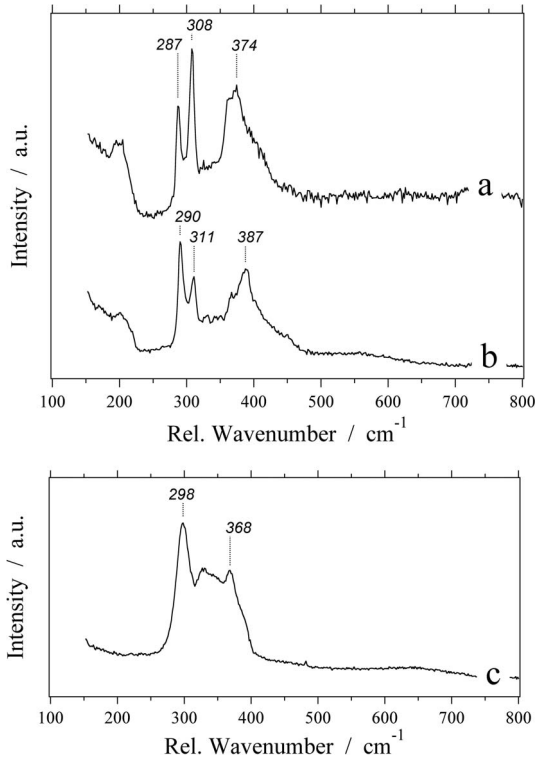

FIG. 6. Raman spectra for PGM from the Svetly Bor dunite. (A) Bowieite $(Rh_{1.16}Ir_{0.82}Cu_{0.02})_{\Sigma 2.00}S_{3.00}$. (B) Kashinite $(Ir_{1.06}Rh_{0.87}Cu_{0.04})_{\Sigma 1.97}S_{3.03}$. (C) Unnamed PGM $(Ir_{0.26}Rh_{0.13}Pt_{0.12}Ni_{0.18}Cu_{0.18}Fe_{0.11})_{\Sigma 0.98}S$. a.u. = arbitrary unit.

garutiite (McDonald *et al*. 2010) and other PGM (Zaccarini *et al*. 2010, Vymazalová *et al*. 2012, 2014). The results presented in this contribution confirm the validity of Raman spectroscopy in the investigation of PGM. However, as the cell parameters and the Raman spectra of bowieite and kashinite are very similar, the ultimate methodology to distinguish them is electron-microprobe analysis.

The unnamed $(Ir_{0.26}Rh_{0.13}Pt_{0.12}Ni_{0.18}Cu_{0.18}Fe_{0.11})_{\Sigma 0.98}S$ phase very likely represents a new PGM. However, its small size, less than 20 μm, prevents us from obtaining X-ray diffraction data to confirm this inference.

According to the worldwide occurrences of bowieite–kashinite compiled in Table 5, with few exceptions, bowieite typically occurs as an inclusion in Pt–Fe alloy associated with Ural-Alaskan type complexes. Kashinite is a common inclusion in chromite crystals of ophiolitic and, to a lesser extent, Ural-Alaskan type chromitites. These observations suggest

TABLE 5. SELECTED WORLDWIDE OCCURRENCES OF BOWIEITE–KASHINITE SERIES

Country	Deposits	Type of Deposits	Host rocks-complex	Assemblage	Ref.
Bowieite					
Australia	Fifield	Placer	UAC	inclusion in Pt-Fe	1, 2
Austria	Kraubath	Lode	LCO	inclusion in chromite	3, 4
Bulgaria	Novoseltsi	Placer	?	?	5
Burma	Chindwin	Placer	Ophiolite	inclusion in Pt-Fe	6
Canada	British Columbia	Placer	UAC	inclusion in Pt-Fe	7
Canada	Burwash creek	Placer	UAC	inclusion in Pt-Fe	8
Canada	Thetford Mines	Lode	BCO	inclusion in chromite	9
China	Gaosital	?	UAC	?	10
Dominican Republic	Loma Peguera	Lode	Ni-laterite	inclusion in chromite	11
Ecuador	Santiago River	Placer	UAC	inclusion in Pt-Fe	12
Ethiopia	Yubdo	Placer	UAC	inclusion in Pt-Fe	13, 14
India	Shimoga	Lode	Layered	inclusion in chromite	15
Madagascar	Manampotsy	Placer	UAC	inclusion in Pt-Fe	16, 17
Mongolia	Burgastain	Placer	UAC	inclusion in Pt-Fe	18
Russia	Svetly Bor	Lode	UAC	inclusion in Pt-Fe	p.w.
Russia	Gusevogorskiy	Lode	?	?	19
Russia	Baimka	Placer	UAC	inclusion in Pt-Fe	20
Russia	Maior River	Placer	UAC	inclusion in Pt-Fe	21
Russia	Miass River	Placer	UAC	inclusion in Pt-Fe	22
Russia	Filippa	Placer	UAC	inclusion in Pt-Fe	23
Russia	Uktus	Placer	UAC	inclusion in Pt-Fe	24
Russia	Anabar basin	Placer	UAC	inclusion in Pt-Fe	25
Sierra Leone	Free Town	Lode	Gabbro	inclusion in magnetite	26
South Africa	Bushveld	Placer	Merensky Reef	inclusion in Pt-Fe	27
USA	Goodnews Bay	Placer	UAC	inclusion in Pt-Fe	28
Kashinite					
Australia	Fifield	Placer	UAC	inclusion in Pt-Fe	1, 2
Austria	Kraubath	Lode	BCO	inclusion in chromite	3, 4
Burma	Chindwin	Placer	?	inclusion in Pt-Fe	6
Cuba	Sagua de Tánamo	Lode	MCO	inclusion in chromite	29
New Caledonia	Pirogue	Lode	LCO	inclusion in chromite	30
Papua New Guinea	Aikora river	Placer	Ophiolite	inclusion in Pt-Fe	31
Russia	Svetly Bor	Lode	UAC	inclusion in Pt-Fe	p.w.
Russia	Ray Iz	Lode	MCO	inclusion in chromite	33, 34
Russia	Nurali	Lode	LC	inclusion in chromite	35
Russia	Uktus	Lode	UAC	inclusion in chromite	24, 36, 37
Russia	Maior River	Placer	UAC	inclusion in Pt-Fe	21
Russia	Filippa	Placer	UAC	inclusion in Pt-Fe	23
Russia	Pana Tundra	Lode	Sulfide	?	38
Turkey	Muğla	Lode	MCO	inclusion in chromite	39
UK	Ballantrae	Lode	MCO	inclusion in chromite	40

p.w. = present work, UAC = Ural Alaskan type, BCO = banded chromitite in ophiolite, MCO = mantle chromitite in ophiolite, LC = lherzolite complex chromitite.

Ref.: 1 = Johan *et al.* 1991, 2 = Slansky *et al.* 1991, 3 = Malitch *et al.* 2001, 4 = Malitch *et al.* 2003, 5 = Atanasov 1990, 6 = Hagen *et al.* 1990, 7 = Barkov *et al.* 2005, 8 = Fedortchouk *et al.* 2010, 9 = Corrivaux & Laflamme 1990, 10 = Chen *et al.* 1981, 11 = Aiglsperger *et al.* 2015, 12 = Weiser & Schmidt-Thome 1993, 13 = Cabri *et al.* 1981, 14 = Stanley *et al.* 2005, 15 = Devaraju *et al.* 2004, 16 = Augé & Legendre 1992, 17 = Legendre and Augé 1992, 18 = Oyunchimeg *et al.* 2009, 19 = Begizov *et al.* 1975, 20 = Gornostayev *et al.* 1999, 21 = Podlipskii *et al.* 1999, 22 = Britvin *et al.* 2001, 23 = Sidorov *et al.* 2004, 24 = Zaccarini *et al.* 2013, 25 = Airiyants *et al.* 2014, 26 = Bowles *et al.* 2013, 27 = Melcher *et al.* 2005, 28 = Desborough & Criddle 1984, 29 = González-Jiménez *et al.* 2011, 30 = Legendre and Augé 1986, 31 = Weiser & Bachmann 1999, 32 = Begizov *et al.* 1985, 33 = Garuti *et al.* 1999, 34 = Pašava *et al.* 2011, 35 = Zaccarini *et al.* 2004, 36 = Garuti *et al.* 2002, 37 = Garuti *et al.* 2003, 38 = Gabov 2010, 39 = Uysal *et al.* 2009, 40 = Power & Pirrie 2004.

that both these PGM can be useful in defining the nature of their source rocks where they occur solely in placer deposits.

Acknowledgments

We are very grateful to the reviewers Bob Martin and Vasilis Tsikouras for constructive comments that improved the manuscript. Many thanks are due to Tania Evstigneeva, Lee A. Groat, and Mackenzie Parker for their editorial handling. The University Centrum for Applied Geosciences (UCAG) is thanked for access to the Eugen F. Stumpfl Electron Microprobe Laboratory. The research was supported by the grant "Progetto d'Ateneo 2013, University of Firenze" to LB and the Russian RFBR grant № 16-05-00508-a to EP.

References

Aiglsperger, T., Proenza, J., Zaccarini, F., Lewis, J., Garuti, G., Labrador, M., & Longo, F. (2015) Platinum group minerals (PGM) in the Falcondo Ni-laterite deposit, Loma Caribe peridotite (Dominican Republic). *Mineralium Deposita* **50**, 105–123.

Airiyants, E.V., Zhmodik, S.M., Ivanov, P.O., Belyanin, D.K., & Agafonov, L.V. (2014) Mineral inclusions in Fe-Pt solid solution from the alluvial ore occurrences of the Anabar basin (northeastern Siberian Platform). *Russian Geology and Geophysics* **55**, 945–958.

Atanasov, A.V. (1990) Vasilite, $(Pd,Cu)_{16}(S,Te)_7$, a new mineral species from Novoseltsi, Bulgaria. *Canadian Mineralogist* **28**, 687–689.

Augé, T. & Legendre, O. (1992) Pt-Fe nuggets from alluvial deposits in eastern Madagascar. *Canadian Mineralogist* **30**, 983–1004.

Barkov, A.Y., Fleet, M.E., Nixon, G.T., & Levson, V.M. (2005) Platinum-group minerals from five placer deposits in British Columbia, Canada. *Canadian Mineralogist* **43**, 1687–1710.

Begizov, V.D., Borisenko, L.F., & Uskov, Y.D. (1975) Sulfides and natural solid solution of platinum metals from ultramafic rocks of the Gusevogorskiy pluton, Urals. *Doklady Akademii Nauk SSSR* **225**, 134–137.

Begizov, V.D., Zabyalov, E.N., Rudashevskii, N.S., & Vyal'sov, L.N. (1985) Kashinite $(Ir,Rh)_2S_3$ – a new sulfide of iridium and rhodium. *Zapiski Vsesouznogo Mineralogicheskogo Obshestva* **114**, 617–622 (in Russian).

Bowles, J.F.W., Prichard, H.M., Suárez, S., & Fisher, P.C. (2013) The first report of platinum-group minerals in magnetite-bearing gabbro, Freetown Layered Complex, Sierra Leone: Occurrences and genesis. *Canadian Mineralogist* **51**, 455–473.

Britvin, S.N., Rudashevsky, N.S., Bogdanova, A.N., & Shcherbachev, D.K. (2001) Miassite $Rh_{17}S_{15}$, a new mineral from a placer of the Miass River, Urals. *Zapiski Vserossiiskogo Mineralogicheskogo Obshchestva* **130(2)**, 41–45 (in Russian).

Cabri, L.J., Criddle, A.J., Laflamme, J.H.G., Bearne, G.S., & Harris, D.C. (1981) Mineralogical study of complex Pt-Fe nuggets from Ethiopia. *Bulletin de Minéralogie* **104**, 508–525.

Chen Keqiao, Shi Nicheng, & Peng Zhizhon (1981) Preliminary study on sulrhodite Rh_2S_3 – a new mineral of platinum group. *Chinese Science Bulletin* **26**, 767–768.

Corrivaux, L. & Laflamme, J.H.G. (1990) Minéralogie des éléments du group du platin dans les chromitites de l'ophiolite de Thetford Mines, Québec. *Canadian Mineralogist* **28**, 579–595.

Desborough, G.A. & Criddle, A.J. (1984) Bowieite: a new rhodium-iridium-platinum sulfide in platinum-alloy nuggets, Goodnews Bay, Alaska. *Canadian Mineralogist* **22**, 543–552.

Devaraju, T.C., Alapieti, T.T., & Kaukonen, R.J. (2004) Geochemistry of ultramafic lenses in the granitoids of the southeastern flanks of Shimoga supracrustal belt (Karnataka) with a note on the distribution of platinum group elements and minerals. *Journal of the Geological Society of India* **63**, 371–386.

Fedortchouk, Y., Lebarge, W., Barkov, A.Y., Fedele, L., Bodnar, R.J., & Martin, R.F. (2010) Platinum-group minerals from a placer deposit in Burwash creek, Kluane area, Yukon territory, Canada. *Canadian Mineralogist* **48**, 583–596.

Gabov, D.A. (2010) PGE and Au minerals from the low-sulfide ore of the Pana Tundra Pluton, Kola Peninsula. *Geology of Ore Deposits* **52**, 624–629.

Garuti, G., Zaccarini, F., Moloshag, V., & Alimov, V. (1999) Platinum-group minerals as indicator of sulfur fugacity in ophiolitic upper mantle: an example from chromitites of the Ray-Iz ultramafic complex (Polar Urals, Russia). *Canadian Mineralogist* **37**, 1099–1115.

Garuti, G., Pushkarev, E., & Zaccarini, F. (2002) Composition and paragenesis of Pt alloys from chromitites of the Uralian-Alaskan-type Kytlym and Uktus complexes, northern and central Urals, Russia. *Canadian Mineralogist* **40**, 1127–1146.

Garuti, G., Pushkarev, E.V., Zaccarini, F., Cabella, R., & Anikina, E.V. (2003) Chromite composition and platinum-group mineral assemblage in the Uktus Alaskan-type complex (Central Urals, Russia). *Mineralium Deposita* **38**, 312–326.

González-Jiménez, J.M., Proenza, J.A., Gervilla, F., Melgarejo, J.C., Blanco-Moreno, J.A., Ruiz-Sánchez, R., & Griffin, W.L. (2011) High-Cr and high-Al chromitites from the Sagua de Tánamo district, Mayarí-Cristal ophiolitic massif (eastern Cuba): constraints on

their origin from mineralogy and geochemistry of chromian spinel and platinum-group elements. *Lithos* **125**, 101–121.

Gornostayev, S.S., Crocket, J.H., Mochalov, A.G., & Laajoki, K.V.O. (1999) The Platinum-group minerals of the Baimka placer deposits, Aluchin horst, Russian Far East. *Canadian Mineralogist* **37**, 1117–1129.

Hagen, D., Weiser, T., & Htay, T. (1990) Platinum-group minerals in Quaternary gold placers in the upper Chindwin area of northern Burma. *Mineralogy and Petrology* **42**, 265–286.

Hansen, M. & Anderko, K. (1958) *Constitution of binary alloys*. McGraw-Hill, New York, New York, United States.

Johan, Z., Slansky, E., & Ohnenstetter, M. (1991) Isoferroplatinum nuggets from Milverton (Fifield, NSW, Australia): a contribution to the origin of PGE mineralization in Alaskan-type complexes. *Comptes Rendus Academie de Sciences Serie II* **312**, 55–60.

Legendre, O. & Augé, T. (1986) Mineralogy of platinum-group mineral inclusions in chromitites from different ophiolitic complexes. *Metallogeny of Basic Ultrabasic Rocks*, 361–372.

Legendre, O. & Augé, T. (1992) Alluvial platinum-group minerals from the Manampotsy area, east Madagascar. *Australian Journal of Earth* Sciences **39**, 389–404.

Malitch, K.N., Melcher, F., & Mühlhans, H. (2001) Palladium and gold mineralization in podiform chromitite at Kraubath, Austria. *Mineralogy and Petrology* **73**, 247–277.

Malitch, K.N., Thalhammer, O.A.R., Knauf, V.V., & Melcher, F. (2003) Diversity of platinum-group mineral assemblages in banded and podiform chromitite from the Kraubath ultramafic massif, Austria: evidence for an ophiolitic transition zone? *Mineralium Deposita* **38**, 282–297.

McDonald, A.M., Proenza, J.A., Zaccarini, F., Rudashevsky, N.S., Cabri, L.J., Stanley, C.J., Rudashevsky, V.N., Melgarejo, J.C., Lewis, J.F., Longo, F., & Bakker, R.J. (2010) Garutiite, (Ni,Fe,Ir), a new hexagonal polymorph of native Ni from Loma Peguera, Dominican Republic. *European Journal of Mineralogy* **22**, 293–304.

Melcher, F., Oberthür, T., & Lodziak, J. (2005) Modification of detrital platinum-group minerals from the eastern Bushveld Complex, South Africa. *Canadian Mineralogist* **43**, 1711–1734.

Oxford Diffraction (2006) *CrysAlis* RED (Version 1.171.31.2) and ABSPACK in *CrysAlis*RED. Oxford Diffraction Ltd., Abingdon, Oxfordshire, England.

Oyunchimeg, T., Izokh, A.E., Vishnevsky, A.V., & Kalugin, V.M. (2009) Isoferroplatinum mineral assemblage from the Burgastain Gol placer (Western Mongolia). *Russian Geology and Geophysics* **50**, 863–872.

Parthé, E., Hohnke, D., & Hulliger, F. (1967) A new structure type with octahedron pairs for Rh_2S_3, Rh_2Se_3 and Ir_2S_3. *Acta Crystallographica* **23**, 832–840.

Pašava, J., Knésl, I., Vymazalová, A., Vavřín, I., Gurskaya, L.I., & Kolbantsev, L.R. (2011) Geochemistry and mineralogy of platinum-group elements (PGE) in chromites from Centralnoye I, Polar Urals, Russia. *Geoscience Frontiers* **2**, 81–85.

Podlipskii, M.Yu., Sidorov, E.G., Tolstykh, N.D., & Krivenko, A.P. (1999) Cobalt-bearing malanite and other Pt-thiospinels from the Maior River placers: (Kamchatka). *Geologiya i Geofizika* **4**, 645–648 (in Russian).

Power, M.R. & Pirrie, D. (2004) Platinum-group minerals within the Ballantrae Complex, SW Scotland. *Scottish Journal of Geol*ogy **40**, 1–5.

Sidorov, E.G., Tolstykh, N.D., Podlipsky, M.Yu., & Pakhomov, I.O. (2004) Placer PGE minerals from the Filippa clinopyroxenite-dunite massif (Kamchatka). *Russian Geology and Geophysics* **45**, 1128–1144.

Slansky, E., Barron, L.M., Suppel, D., Johan, Z., & Ohnenstetter, M. (1991) Platinum mineralization in the Alaskan-type intrusive complexes near Fifield, N.S.W., Australia. Part 2. Platinum-group minerals in placer deposits at Fifield. *Mineralogy and Petrology* **43**, 161–180.

Stanley, C.J., Criddle, A.J., Spratt, J., Roberts, A.C., Szymański, J.T., & Welch, M.D. (2005) Kingstonite, $(Rh,Ir,Pt)_3S_4$, a new mineral species from Yubdo, Ethiopia. *Mineralogical Magazine* **69**, 447–453.

Turrel, G. (1996) The Raman effect. *In* Raman microscopy: Developments and application (G. Turrel & J. Corset, eds.). Elsevier Academic Press, Amsterdam, Netherlands (2–25).

Uysal, I., Tarkian, M., Sadiklar, M.B., Zaccarini, F., Meisel, T., Garuti, G., & Heidrich, S. (2009) Petrology of Al- and Cr-rich ophiolitic chromitites from the Muğla, SW Turkey: implications from composition of chromite, solid inclusions of platinum-group mineral, silicate, and base-metal mineral, and Os-isotope geochemistry. *Contribution to Mineralogy and Petrology* **158**, 659–674.

Vymazalová, A., Laufek, F., Drábek, M., Stanley, C.J., Bakker, R.J., Bermejo, R., Garuti, G., Thalhammer, O., Proenza, J.A., & Longo, F. (2012) Zaccariniite, RhNiAs, a new platinum-group mineral from loma peguera, Dominican Republic. *Canadian Mineralogist* **50**, 1321–1329.

Vymazalová, A., Zaccarini, F., & Bakker, R.J. (2014) Raman spectroscopy characterisation of synthetic platinum-group minerals (PGM) in the Pd–Sn–Te and Pd–Pb–Te ternary systems. *European Journal of Mineralogy* **26**, 711–716.

Weiser, T.W. & Bachmann, H.G. (1999) Platinum-group minerals from the Ankora river area, Papua New Guinea. *Canadian Mineralogist* **37**, 1131–1145.

Weiser, T. & Schmidt-Thomé, M. (1993) Platinum-group minerals from the Santiago River, Esmeraldas Province, Ecuador. *Canadian Mineralogist* **31**, 61–73.

Yefimov, A.A., Yefimova, L.P., & Maegov, V.I. (1993) The tectonics of the platinum-bearing belt of the Urals: composition and mechanism of structural developments. *Geotectonics* **27**, 197–207.

Zaccarini, F., Pushkarev, E., Fershatater, G., & Garuti, G. (2004) Composition and mineralogy of PGE-rich chromitites in the Nurali lherzolite-gabbro complex, southern Urals. *Canadian Mineralogist* **42**, 545–562.

Zaccarini, F., Bakker, R.J., Garuti, G., Aiglsperger, T., Thalhammer, O.A.R., Campos, L., Proenza, J.A., & Lewis, J. (2010) Platinum group minerals in chromitite of Costa Rica: mineralogical characterization by electron microprobe and Raman-spectroscopy. *Boletin de la Sociedad Geologica Mexicana* **61**, 161–171.

Zaccarini, F., Pushkarev, E., Garuti, G., Krause, J., Dvornik, G.P., Stanley, C., & Bindi, L. (2013) Platinum-group minerals (PGM) nuggets from alluvial-eluvial placer deposits in the concentrically zoned mafic-ultramafic Uktus complex (Central Urals, Russia). *European Journal of Mineralogy* **25**, 519–531.

Received February 7, 2015. Revised manuscript accepted April 1, 2015.